Regnase-1 deficiency restrains *Klebsiella pneumoniae* infection by regulation of a Type I interferon response

Running title: Loss of Regnase-1 promotes resilience to *Klebsiella pneumoniae*

Giraldina Trevejo-Nuñez[a#], Becky Lin[a], Li Fan[b], Felix E. Y. Aggor[c], Partha S. Biswas[c], Kong Chen[b], and Sarah L. Gaffen[c]

[a]Division of Infectious Diseases, University of Pittsburgh School of Medicine, Pittsburgh, Pennsylvania, USA

[b]Division of Pulmonary, Allergy and Critical Care Medicine, University of Pittsburgh School of Medicine, Pittsburgh, Pennsylvania, USA

[c]Division of Rheumatology and Clinical Immunology, University of Pittsburgh School of Medicine, Pittsburgh, Pennsylvania, USA

[#]Corresponding author: Giraldina Trevejo-Nuñez, MD

giraldina.trevejo@pitt.edu

Graphical abstract

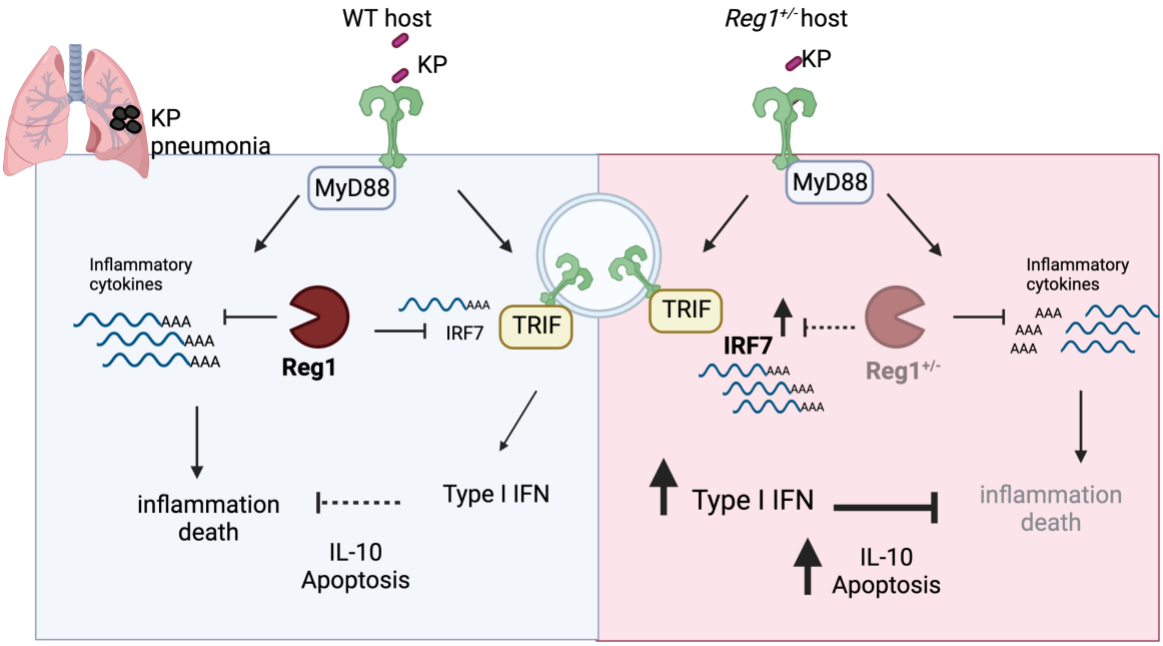

Abstract

Excessive inflammatory responses can cause collateral tissue damage or autoimmune inflammation, sometimes with severe morbidity or mortality. During host defense responses, numerous negative feedback mechanisms are established to prevent excessive unchecked inflammation. However, this restraint can sometimes come at the cost of suboptimal infection control, and we do not fully understand how this balance is maintained during different infection settings. The endoribonuclease Regnase-1 (Reg1, Zc3h12a, MCPIP1) is an RNA binding protein (RBP) that binds and degrades many target mRNA transcripts. Reg1 is a potent feedback regulator of IL-17 and LPS signal transduction, among other stimuli. Consequently, Reg1 deficiency exacerbates autoimmune inflammation in multiple mouse models, but on the other hand, reduced Reg1 improves immunity to fungal infection. To date, the role of Reg1 in bacterial immunity is poorly defined. Here, we show that mice deficient in Reg1 are more resistant to pulmonary *Klebsiella pneumoniae* (KP) infection. Unexpectedly, effects of Reg1 deficiency were not due to accelerated eradication of bacteria or increased pro-inflammatory cytokine expression. Rather, alveolar macrophages from Reg1-deficient mice showed enrichment of Type I IFN-related genes upon KP infection, accompanied by increased Ifnb1 expression. Surprisingly, the stability of Ifnb1 mRNA was not altered by Reg1-deficiency; rather, mRNA encoding its upstream regulator IRF7 appeared to be a more prominent target. Blockade of IFNR during KP infection reversed disease improvement. Thus, impaired Reg1 induces Type I IFN and enhances resistance to KP, raising the possibility that Reg1 could be a potential clinical target in acute bacterial infections.

41 **Introduction**

42 *Klebsiella pneumoniae* (KP) is a constituent of the normal human normal human
43 microbiome and is detected in approximately 10% of the Human Microbiome Project samples (1,
44 2). KP is the third most common cause of ventilator-associated pneumonia (VAP) in the USA, and
45 its presence correlates with prolonged duration of ventilation and ICU hospital stay (3-5). KP
46 imposes a major infectious disease challenge due to increasing antimicrobial resistance combined
47 with comparatively limited therapeutic options (6). Hence, an improved understanding of host-
48 pathogen interactions is needed to elucidate, and ultimately exploit, the host mechanisms that
49 control KP pneumonia.

50 The immune response to infectious pathogens is finely balanced to allow eradication of
51 microbes yet still prevent excessive inflammatory pathology. Thus, numerous mechanisms are
52 triggered during immune responses to counter-regulate deleterious responses and thereby
53 minimize collateral damage to the host. The RNA-binding protein (RBP) Regnase-1 (Reg1), also
54 known as MCP1-induced protein 1 (MCPIP1), is encoded by the *ZC3H12A* gene and has intrinsic
55 endoribonuclease activity that keeps inflammatory responses in check (7). In this capacity, Reg1
56 binds and degrades many mRNA transcripts, including its own mRNA, through recognition of
57 characteristic stem-loop secondary structures in the 3' untranslated region (UTR) of target mRNAs
58 (8). Reg1 is induced by many inflammatory stimuli, including IL-1, Toll-like-receptors (TLR) and
59 IL-17 (9-12). In addition, TCR signaling leads to cleavage of Reg1, releasing T cells from Reg1-
60 mediated suppression (13). Thus, Reg1 plays a central role in negative feedback control of pro-
61 inflammatory cytokine gene expression through post-transcriptional control of mRNA expression.

62 Multiple mouse models support the vital role of Reg1 as a central negative regulator of
63 pathogenic inflammation. Reg1 knockout mice (*Zc3h12a*$^{-/-}$, here called *Reg1*$^{-/-}$) have a life span

64 only of 6-8 weeks. *Reg1*$^{-/-}$ mice display significant constitutive inflammation, manifesting as
65 growth retardation, splenomegaly, lymphadenopathy, heightened systemic and localized cytokine
66 production, and ultimately multi-organ failure (9, 14). In order to avoid confounding issues with
67 the complete Reg1 knockout mouse, we have previously taken advantage of *Reg1* heterozygous
68 mice (*Reg1*$^{+/-}$), which have normal life spans and fertility, normal tonic expression of Reg1, and
69 minimal peripheral organ inflammation at baseline (11, 15). Even so, cells from *Reg1*$^{+/-}$ mice
70 display markedly reduced Reg1 expression after LPS or IL-17 stimulation, and tissues from
71 *Reg1*$^{+/-}$ animals (lung, kidney, central nervous system) exhibit elevated cytokine responses (11).
72 Consequently, *Reg1*$^{+/-}$ mice show exacerbated signs of autoimmunity in multiple IL-17-driven
73 autoimmune conditions, including experimental autoimmune encephalomyelitis (EAE),
74 imiquimod (IMQ)-induced dermatitis and autoantibody-induced glomerulonephritis (AGN). In all
75 these settings, IL-17R deficiency reversed the phenotype, demonstrating that Reg1 functions in
76 these settings through restricting IL-17-driven inflammation (11, 15, 16).

77 In contrast to exacerbating pathology in autoimmune conditions, Reg1-deficiency leads to
78 improved resistance to at least one IL-17-mediated host response, disseminated candidiasis,
79 causing enhanced survival and concomitantly reduced fungal kidney burdens (11). Therefore,
80 although restraint of Reg1 is clearly beneficial to limit autoimmune pathology, it is conceivable
81 that temporary blockade of Reg1 could be exploited to improve inflammatory immune responses
82 during certain infectious settings. However, the impact of Reg1 in infectious disease settings has
83 not been extensively explored.

84 KP is sensed by pattern recognition receptors such as TLR4, which activates a myeloid
85 differentiation primary response gene 88 (MyD88)-dependent pathway leading to induction of pro-
86 inflammatory chemokines and cytokines. TLR4 signaling also induces the TIR-domain-containing

87 adaptor-inducing interferon-β (TRIF) pathway, which induces of Type I IFNs (IFN-α, IFN-β).
88 Both MyD88 and TRIF signaling pathways are needed for defense against KP infection (17, 18).
89 TLR4 is also upstream of IL-17 production from γδ T cells in response to KP (19), and *Il17ra*$^{-/-}$
90 mice have uncontrolled KP infection with associated decreased expression of CXC chemokines,
91 G-CSF and impaired neutrophil recruitment (20). Additionally, IL-17 synergizes with cytokines
92 such as IL-22 to increase production of antimicrobial peptides in lung epithelium, such as LCN2,
93 calprotectin (S100A8/9) and MUC1(21). Though produced by lymphocytes, IL-17 mediates
94 downstream signals selectively on non-hematopoietic cells within the pulmonary epithelium
95 during KP infection (22). Thus, the TLR4 and IL-17R pathways mediate an integrated
96 inflammatory cascade that contains KP lung infection.
97 Given the documented role of Reg1 in restricting both TRL4- and IL-17-dependent
98 signaling pathways, we hypothesized that Reg1-deficiency would be protective in the context of
99 KP pneumonia, likely through decreased decay of pro-inflammatory mRNA transcripts. Indeed,
100 we find here that Reg1-deficiency renders mice resistant to KP. However, bacterial burdens and
101 typical pro-inflammatory cytokines known to be targeted by Reg1 were not altered in Reg1-
102 deficent mice. Gene profiling of alveolar macrophages from KP-infected mice showed striking
103 enrichment of type I IFN-associated gene pathways during Reg1 deficiency. Consistent with this,
104 blockade of IFNR signaling reversed the protective effects of Reg1 deficiency. Mechanistically,
105 Reg1 regulated the stability of mRNA encoding IRF7, an upstream regulator of Type 1 IFN gene
106 expression by TLRs.
107

108 **Material and Methods**

109 ***Mice***

110 *Reg1*$^{+/-}$ and *Reg1*$^{+/+}$ *(Zc3h12a)* littermates on the C57BL/6 background were co-housed and used
111 for all experiments. *Reg1(Zc3h12a)*$^{fl/fl}$ mice are under material transfer agreement (MTA) from
112 University of Central Florida (Orlando, Florida, USA). *Sftpc*^{Cre} mice and CD45.1 mice were from
113 The Jackson Laboratory. Mice were 8-12-weeks old and both sexes were used. All animal studies
114 were approved by the Institutional Animal Care and Use Committee (IACUC) of the University
115 of Pittsburgh.

116

117 ***Bacterial infections and anti-IFNR1 treatment***

118 KP ATCC strain 43816 was grown in tryptic soy broth to reach early log phase. 1-2x10^3
119 CFU/mouse in PBS was administered by deep oropharyngeal aspiration. Where indicated,
120 tamoxifen (TAM) was administered i.p. at 75 mg/kg dissolved in corn oil for 5 d and then rested
121 for 5 d prior to induction of infection. *Reg1*$^{+/-}$ mice were treated with anti-IFNR1 antibodies or
122 isotype control by i.p injection (Bio-Xcell MAR1-5A3, 250 ug/mouse, administered on Day 0 and
123 Day 2 p.i). Mice were followed for 7 days.

124

125 ***Bone marrow chimeras***

126 WT (CD45.1) and *Reg1*$^{+/-}$ (CD45.2) mice were lethally irradiated (900 Gy). After 24h, each mouse
127 received 4x10^6 bone marrow cells by tail vein injection. Mice received antibiotics in drinking water
128 starting 1 d before irradiation and continued for 10 d (trimethroprim/sulfametoxazole 200/40 mg).
129 After 6 weeks, engraftment was confirmed by flow cytometry of blood for CD45.1 and CD45.2
130 markers.

131 ***Bacterial burden, mRNA, and protein analysis***

132 Tissues were homogenized in PBS and CFU levels were assessed by serial dilution plating. Lung
133 tissues were homogenized in TrIzol (Invitrogen) and subjected to qPCR with SybrGreen probes.
134 Threshold cycle (C_T) values were normalized to *Gapdh.* ELISA kits were from eBioscience
135 (Thermo Fisher Scientific) and R&D Systems. Abs used in western blots were cleaved caspase-3,
136 total caspase 3 (Cell Signaling) and beta-actin (Abcam).

137

138 ***Flow cytometry***

139 Lungs were digested with lung dissociation kits (Miltenyi). Lung cell suspensions were stained for
140 CD45, LyG, CD11b, CD11c, SiglecF, Ly6C, CD3, CD4, NK1.1, IFN-γ. Abs were from
141 eBioscience, BD Biosciences or Biolegend. Alveolar macrophages ($CD45^+$, LyG^- $CD11b^-$
142 $CD11c^{hi}$, $SiglecF^+$) were isolated by FACS. Proliferation was assessed by BrDU incorporation
143 (BD Biosciences); briefly, mice were injected i.p. with 1 mg of BrDU one day before sacrifice.
144 Data were acquired on LSR Fortessa and analyzed with FlowJo software.

145

146 ***Bone marrow derived macrophages (BMDM)***

147 BM cells were extracted from *Reg1*$^{+/-}$ and *Reg1*$^{+/+}$ mice femur and tibia and differentiated into
148 BMDM with L929 media (30%) for 5-6 days. Cultured BMDMs were stimulated with heat-killed
149 KP (MOI = 10) up to 8 h or *Klebsiella* LPS (1 ug/ml) (Sigma-Aldrich).

150

151 ***RNA Sequencing and Analysis***

152 Samples from 12 individual mice (uninfected *Reg1*$^{+/+}$ n=3, uninfected *Reg1*$^{+/-}$ n=3, KP-infected
153 *Reg1*$^{+/+}$ n=4, KP-infected *Reg1*$^{+/-}$ n=4) were used . Mice were infected with KP by oropharyngeal

154 aspiration. After 24 h, alveolar macrophages were stained as described above and sorted by flow
155 cytometry with a purity of 99%. Cells were placed into RLT-plus (Qiagen, Valencia, CA) and total
156 RNA extracted using RNeasy MiniKits (Qiagen). RNA was quantitated using Nanodrop and
157 integrity determined with a total RNA Nano Chip (Agilent Technologies). Single-stranded total
158 RNA-seq libraries were sequenced with an Illumina Nextseq500 sequencer with a depth of
159 25 million reads per sample (75 bp single-end) at the University of Pittsburgh Health Sciences
160 Sequencing Core. Fastq files with high quality reads (phred score >30) were uploaded to the CLC
161 Genomics Workbench (Qiagen) and reads aligned to the mouse reference genome. Transcript
162 counts and differential expression analyses were carried out using the CLC Genomics Workbench.
163 RNAseq data were deposited to Sequence Read Archive (SRA), BioProject ID: PRJNA789160.
164

165 ***Lung Histology***

166 Lungs from *Reg1*$^{+/-}$ and *Reg1*$^{+/+}$ mice isolated at 48 h p.i. were fixed in 10% neutral buffered
167 formalin for 24 h. Sections were stained with hematoxylin and eosin (H&E) by the University of
168 Pittsburgh histology core. Slides were visualized on an EVOS microscope. Lung damage
169 parameters measured were: A) Parenchymal inflammation and percentage of compromised tissue,
170 B) peribronchial, and C) perivascular inflammation. The assigned score values were 0) none, 1)
171 <25%, 2) 25-50%, 3) 50-75%, 4) >75%.
172

173 ***Statistical Analysis***

174 Data were analyzed on Prism (GraphPad). Data were analyzed by Log-Rank, One-way analysis of
175 variance (ANOVA), Student's t test, and post hoc tests were used as indicated. Each symbol
176 represents one mouse unless indicated.

177
178 **Results**
179

180 ***Reg1-deficient mice are resistant to KP lung infection***

181 A complete absence of Reg1 is extremely deleterious, as Reg1$^{-/-}$ mice exhibit severe
182 inflammation and severely shortened life spans (9). In contrast, *Reg1*$^{+/-}$ mice (sometimes termed
183 here Reg1-deficient) have a normal life span without peripheral organ inflammation.
184 Nonetheless, *Reg1*$^{+/-}$ mice show enhanced pro-inflammatory responses in multiple IL-17-driven
185 autoinflammatory model settings (11, 15, 16). To determine whether Reg1 haploinsufficiency
186 influences immunity to KP infection, *Reg1*$^{+/-}$ and *Reg1*$^{+/+}$ littermate controls were infected with
187 KP by oropharyngeal aspiration. Survival and parameters of health including weight loss were
188 monitored over time. Indeed, infection-induced survival and weight loss were significantly
189 ameliorated in Reg1-deficient mice compared to *Reg1*$^{+/+}$ littermate controls (**Fig. 1A, B**).
190 Unexpectedly, this improvement in survival was not accompanied by statistically significant
191 differences in lung bacterial burdens (**Fig 1C**). Moreover, there were no changes in bacterial
192 dissemination into the spleen between groups at any measured time point, even though *Reg1*$^{+/-}$
193 mice had lower expression of Reg1 (*Zc3h12a*) than controls **(Fig. 1D, E).** Furthermore,
194 histologic analysis of infected lung tissues between *Reg1*$^{+/+}$ and *Reg1*$^{+/-}$ animals, showed that
195 *Reg1*$^{+/-}$ mice developed smaller foci of pneumonia compared to controls, with particularly
196 reduced levels of parenchymal inflammation (**Fig. 1F**, **G**). These data suggest that factors other
197 than bacterial burden underlie the improved survival of Reg1-deficient animals.
198

199 ***Reg1 functions in both hematopoietic and non-hematopoietic compartments during KP***
200 ***pneumonia***

201 Reg1 has been shown to act in multiple cell types, including T cells, macrophages and
202 epithelial cells (7, 23). Of relevance to KP, Reg1 can restrict signaling by both TLR4 and IL-
203 17. Whereas TLR4 acts predominantly on hematopoietic cells (especially macrophages), IL-17
204 predominantly mediates signaling in epithelial and/or mesenchymal target tissues,
205 demonstrated in many settings including KP-infected lung (24). As a first step to define the
206 essential compartments in which Reg1 functions to limit immunity to pulmonary KP infection,
207 we used an adoptive transfer approach. Femoral bone marrow (BM) from *Reg1*$^{+/-}$ (CD45.2) or
208 WT (CD45.1) mice were transferred into reciprocal irradiated *Reg1*$^{+/-}$ or WT recipients. After
209 8 weeks, engraftment was confirmed by flow cytometry (data not shown). Successfully
210 reconstituted mice were infected with KP by oropharyngeal aspiration and followed up to 7 days.
211 As expected, WT mice that received WT BM cells were susceptible to KP, whereas *Reg1*$^{+/-}$ mice
212 receiving *Reg1*$^{+/-}$ BM were more resistant. As shown, *Reg1*$^{+/-}$ or WT mice that received *Reg1*$^{+/-}$
213 BM cells were resistant to KP, with almost 80% survival at day 7 post-infection. Additionally,
214 *Reg1*$^{+/-}$ mice that received WT BM cells were resistant to KP, showing 60% survival at day 7
215 (**Fig 2A**). Thus, Reg1 appears to act in multiple compartments.

216 Loss of IL-17RA in pulmonary epithelial cells renders mice highly susceptible to KP
217 infection (24). Accordingly, given the potent impact of Reg1 on IL-17 signaling seen in prior
218 studies (11, 12, 15, 25), we crossed *Reg1*$^{fl/fl}$ to surfactant protein C (*Sftpc*)^{Cre} mice in order to delete
219 Reg1 conditionally in distal pulmonary epithelial cells (distal bronchi and alveoli). As shown, mice
220 were modestly more resistant to KP than controls, though the improvement survival was much less
221 profound than seen in *Reg1*$^{+/-}$ mice (**Fig 2B**), which is consistent with the BM chimera data

222 showing contributions from both the hematopoietic and non-hematopoietic compartments
223 contribute upon KP infection.
224
225 ***Reg1 deficiency does not influence immune cell recruitment or proliferation during KP***
226 ***infection***
227 Based on these data, it is evident that a Reg1 deficiency in the hematopoietic
228 compartment provides a survival advantage to the host. We saw increased percentage of
229 alveolar macrophages at 72h post-infection (**Fig. 3A**). However, there were no changes in the
230 absolute numbers of recruited myeloid cells between *Reg1*$^{+/-}$ and control mice at 48 h and 72
231 h post-infection (**Fig 3B**). Consistent with this, expression of myeloid-recruiting chemokines
232 such as *Cxcl1, Cxcl5* and *Ccl2* were similar among groups, despite the fact that these are all
233 known transcriptional targets of Reg1 in other settings (**Fig. S1A**) (26, 27). There were also no
234 differences in cellular proliferation and macrophage bacterial killing between *Reg1*$^{+/-}$ and
235 control mice (**Fig 3B, C**). It is known that Reg1 controls B cell homeostasis and that complete
236 Reg1 deletion in B cells increases antibody secretion (28). However, IgM and IgA levels in
237 BALF and lung tissue were comparable between *Reg1*$^{+/-}$ and control mice (**Fig 3D**). Taken
238 together, these data suggest that differences in survival during KP infection in *Reg1*$^{+/-}$ mice is
239 not explained by altered recruitment of myeloid cells, cellular proliferation, macrophage killing
240 capacity, or a B cell antibody response.
241
242 ***Resistance to KP caused by Reg1 deficiency is linked to increased interferon (IFN) signature***
243 To understand the mechanisms by which Reg1 deficiency promotes survival, we
244 performed transcriptomic profiling of purified alveolar macrophages from *Reg1*$^{+/-}$ and

245 littermate control lungs at 24 h post-KP infection. This time point was chosen to define the early
246 events that are operative during the initial stages of infection. There were 796 differentially
247 expressed genes, of which 237 were upregulated and 559 were downregulated. Gene set
248 enrichment analysis (GSEA) revealed major changes in type I IFN-related responses (IFN-α),
249 oxidative phosphorylation, and IFN-γ response as the top three enriched gene sets, with a
250 normalized enrichment score (NES) <2.5 for the type I IFN group (**Fig. 4A, B**).

251 We next validated these pathways by functional analysis. Consistent with the RNASeq
252 data, Type I IFN (IFN-β) expression was higher in lung homogenates of Reg1-deficient mice
253 compared to controls at 24 h and 48 h post-infection **(Fig 5A**). Since IFN-β can be produced by
254 macrophages during Gram-negative pneumonia (29), we stimulated *Reg1*$^{+/-}$ or control BMDMs
255 with heat-killed KP and assessed *Ifnb1* mRNA. Indeed, *Ifnb1* was elevated in Reg1-deficient
256 macrophages compared to controls as early as 2 h post-infection (**Fig. 5B**). In contrast, IFN-γ
257 expression was similarly expressed between *Reg1*$^{+/-}$ and Reg1$^{+/+}$ mice after KP infection
258 (**Fig 5C**). Similarly, oxidative phosphorylation, of sorted alveolar macrophages assessed by
259 mitochondrial respiration, was not different between *Reg1*$^{+/-}$ mice and controls (**Fig. S1B,C**).
260 Collectively, these data indicate that Reg1 deficiency induces IFN-β upon KP infection.

261 Reg1 functions primarily by promoting endonucleolytic decay of target mRNA
262 transcripts (30). Based on the observed increased *Ifnb1* expression in Reg-deficient BMDMs,
263 we hypothesized that Reg1 deficiency may result in prolonged stabilization of *Ifnb1* mRNA or
264 regulatory factors upstream of *Ifnb1* regulation. To test this, *Reg1*$^{+/-}$ and control BMDMs were
265 stimulated with LPS to prime expression of genes in the IFN pathway. Cells were treated with
266 actinomycin D (Act D) to block further transcription, and the half-life of candidate target
267 transcripts was assessed over a 2-hour time course. Although the intrinsic mRNA stability of *Ifnb1*

268 or other mRNAs was not detectably altered in Reg1-deficient cells, the half-life of *Irf7* mRNA
269 considerably increased in the setting of Reg1 deficiency (**Fig. 5D**), potentially explaining the
270 increased IFN-β seen in Reg-1 deficient mice upon KP pneumonia.

271 To determine whether Type I IFN accounted for the prolonged survival in *Reg1*$^{+/-}$ mice,
272 we administered anti-IFNR1 Abs or isotype controls at Day 0 and 2 post-KP infection and
273 followed mice for 7 days. Strikingly, 100% of *Reg1*$^{+/-}$ mice that received isotype control Abs
274 survived, while 60% of *Reg1*$^{+/-}$ mice that received anti-IFNR1 succumbed (**Fig. 6**). Therefore,
275 the protection afforded by Reg1-deficiency requires Type I IFN signaling.

276

277 ***Increased Ifnb1 correlates with enhanced anti-inflammatory response in Reg1-deficient mice***

278 IFN-β has the capacity to exert anti-inflammatory effects in the host, reported in several
279 disease models. This effect has been attributed in part to type I IFN induction of IL-10, which
280 dampens expression of transcription of cytokines such as *Tnfa, Cxcl1, Il6* (31, 32). Based on
281 this, we assessed IL-10 in lung homogenates of KP-infected mice. There was a trend to
282 increased IL-10 at 72 h post-infection in *Reg1*$^{+/-}$ mice compared to control mice, though this
283 did not reach statistical significance (**Fig 7A**). TNF-α was not affected *Reg1*$^{+/-}$ compared to
284 controls (**Fig 7B**). We then asked whether apoptosis was affected in *Reg1*$^{+/-}$ mice compared to
285 controls. As shown, cleaved caspase 3 expression in total lung homogenates was increased in
286 *Reg1* $^{+/-}$ mice compared to controls (**Fig 7C, D**). These data suggest that increased IFN-β arising
287 from Reg1 deficiency may confer an anti-inflammatory advantage to *Reg1*$^{+/-}$ mice sufficient to
288 prolong survival upon KP infection.

289

290 **Discussion**

291 Reg1 controls the inflammatory response by degrading many individual inflammatory
292 cytokine mRNAs, including *Il6, Il1b,* and *Il12b,* thus tempering the overall inflammatory milieu
293 (9). Perhaps even more significantly, Reg1 degrades transcripts encoding inflammatory
294 transcription factors (TF) such as *Nfkbiz,* which encodes the non-canonical TF IκBξ, and therefore
295 Reg1 can indirectly affect all IκBξ-inducible genes (11). Thus, it is not unexpected that a complete
296 knockout of Reg1 gene (*Zc3h12a*) is fatal due to severe autoinflammation. *Reg1*$^{+/-}$ mice, on the
297 other hand, appear to have a normal life span, fertility, and do not exhibit peripheral baseline
298 inflammation. However, *Reg1*$^{+/-}$ mice still have an enhanced inflammatory response, particularly
299 when the disease model relies heavily on the IL-17R pathway (11, 15, 25). In this KP infection
300 model, we were surprised that levels of inflammatory cytokines and chemokines were similar
301 between Reg1-deficient mice and controls. Since these mice are haploinsufficient for the Reg1
302 gene (*Zc3h12a*), and KP is sensed by TLR4, one potential explanation is the remaining Reg1 levels
303 may be enough to compensate for the cytoplasmic MyD88-driven pathway, but not the endosomal
304 TRIF-dependent pathway, thus leading to increased type I IFN expression and protection from KP.

305 Since most pro-inflammatory genes known to be driven by Reg1 were unchanged in lung
306 tissues regardless of Reg1 deficiency, and there was a clear increase in the percentage of alveolar
307 macrophage (AM) recruitment, we performed RNAseq in AMs cells in order to evaluate
308 macrophage-intrinsic activities underlying the Reg1-deficient phenotype. This approach has the
309 caveat that contributions from other cells such as interstitial macrophages, inflammatory
310 monocytes or other immune cells may be missed. In this regard, CCR2^{+} inflammatory monocytes
311 recruited during KP infection are known to enhance IL-17 production from ILC3 cells leading to
312 KP eradication (33, 34). However, this mechanism has been shown to be important with clinical

313 strains of KP and not with the serotype used here (ATCC 43816). Future studies will focus on
314 additional cell types to determine more broadly where Reg1 is operative in this setting.

315 The role of type I interferons (IFN-α/IFN-β) in bacterial infections is not fully defined,
316 especially when compared to its extensively-studied roles in viral infections. Even among bacterial
317 pathogens, the response to type I IFN differs depending on site of infection and pathogen
318 characteristics. For instance, type I IFN is detrimental in animal models of *Staphylococcus aureus*
319 and *Listeria monocytogenes* (35, 36). On the other hand, there is a protective response in models
320 of *Legionella pneumophilia* and *Streptococcus pyogenes (37).* In the case of *Klebsiella*
321 *pneumoniae,* IFN-β signaling in NK cells enhances secretion of IFN-γ, decreasing bacterial burden
322 (38). In this study, we did not see differences in recruitment of NK cells or enhanced IFN-γ
323 secretion by NK cells in *Reg1*$^{+/-}$ mice compared to controls. However, the enhanced mortality in
324 control WT mice is significantly decreased in *Reg1*$^{+/-}$ mice, which we propose is due to increased
325 type I IFN that modulates the inflammatory response enough to facilitate bacterial eradication and
326 pneumonia resolution, and this model is supported by histological evidence as well as the
327 observation that anti-IFNR1 blockade reverses the protection provided by Reg1 deficiency.

328 IFN-β can lead to many complex events in bacterial infections, including increased
329 apoptosis, macrophage efferocytosis and resolution of infection in models of *E. coli* pneumonia
330 and peritonitis, associated with enhanced IL-10 secretion (29). IL-10 mediates many anti-
331 inflammatory effects and regulates metabolic reprograming of macrophages (39). Related to this,
332 interstitial macrophages have immunoregulatory properties by secreting IL-10 upon LPS and
333 CPG-DNA stimulation in models of asthma (40). Although there was only a modest trend of
334 increased IL-10 in these settings, there was a clear increase in cleaved Caspase-3 in Reg1-deficient
335 lungs, correlating with increased IFN-β and resistance to KP pneumonia. Concomitantly,

336 transcriptomic profiles revealed several IFN-stimulated genes (ISGs) implicated in regulating
337 apoptosis, including *Ifit2, Ifit3* and *Ifitm3*. Intriguingly, IFIT2 is an RBP that enhances apoptosis
338 (41, 42), though its precise role in the context of Reg1 immunoregulation is as yet unknown. Thus,
339 we speculate one mechanism underlying these results is through actions of type I IFN mediating
340 increases in apoptosis, an important step for resolution of pneumonia (43).

341 Since IFN-β levels were increased in Reg1-deficient mice upon KP infection, we initially
342 expected that Reg1 deficiency would result in enhanced stability of the *Ifnb1* transcript. However,
343 our data instead indicate that the impact on *Ifnb1* appears to be indirect via control of its upstream
344 regulator *Irf7* mRNA, opening a new facet of how Reg1 influences immune responses. A
345 deficiency in a related RBP, Regnase-3 (*Zc3h12c*) also leads to increased IFN (type I and II)
346 signaling, and IRF7 can transcriptionally control expression of Regnase-3 (44). However, Reg3
347 expression was not altered in AMs based on the RNAseq data or in total lung by qPCR, and thus
348 we believe this axis is not a major driver of the effects seen here (**Fig. S2D**).

349 The Type III interferons have emerged in recent years as key regulators of antiviral and
350 antifungal immunity (45). It has been shown that IFN-lambda (L) increases lung epithelial
351 permeability and facilitates bacterial transmigration in animal models infected with KP (KP
352 ST258), an effect that is counteracted by IL-22 (46). In this model we did not see increases in IFN-
353 L despite increase of type I IFN and in vitro stability of IRF-7, though determining whether this
354 axis of interferon activity contributes in any way will require further study (**Fig. S2C**).
355 Surprisingly, though IL-22 and IL-17 signaling are well described to play important roles in KP
356 eradication (20, 21, 24), their expression was also not altered by Reg1 deficiency (**Fig. S2A,B**).
357 This would be consistent with activities of Reg1 being downstream of these or other cytokines

358 rather than upstream of their production, though further analyses will be required to prove that
359 point definitively.

360 The immune system has evolved to balance the vital effects of anti-microbial effector
361 functions with the potential for causing collateral tissue damage. In this regard, the activation of
362 every immune signaling pathway is accompanied by negative feedback signaling events that
363 restrain inflammation (47, 48). In selected conditions, however, it may be clinically beneficial to
364 allow more fulminant inflammation in order to treat a life-threatening condition. Indeed,
365 checkpoint inhibitor blockade for cancer therapy is built on exploiting this concept (49). By
366 analogy, releasing inflammatory "brakes" may be useful in the context of severe infections such
367 as bacterial pneumonia, and the present data suggest that Reg1 could, in principle at least, be one
368 such target.

369

Acknowledgements

GTN was supported by NIH grants HL135476, HL154231, AI153549. KC was supported by HL137709. SLG was supported by AI147383. We thank BM Coleman for technical support and JK Kolls for helpful discussions. We thank the reviewers for excellent suggestions that significantly improved the mansucript.

Abbreviations: AM, alveolar macrophage, BM, bone marrow; BMDM, bone marrow-derived macrophages; KP, *Klebsiella pneumoniae*; MCPIP1, MCP1-induced protein 1 (alternative name for Regnase-1); MyD88, myeloid differentiation primary response gene 88; RBP, RNA binding protein; Reg1, regnase-1; TAM, tamoxifen; TLR, Toll-like receptor; UTR, untranslated region; VAP, ventilator-associated pneumonia

Author contributions

Conceptualization – GTN, PSB, SLG, KC

Investigation – GTN, BL, LF, FEYA, KC

Writing – GTN, SLG

Reviewing and Editing – GTN, KC, PSB, SLG

Visualization – GTN

Supervision – GTN, SLG, PSB

Funding Acquisition – GTN, SLG, KC, PSB

392 **References**

393

394 1. Conlan S, Kong HH, Segre JA. 2012. Species-level analysis of DNA sequence data from
395 the NIH Human Microbiome Project. PLoS One 7:e47075.

396 2. Martin RM, Cao J, Brisse S, Passet V, Wu W, Zhao L, Malani PN, Rao K, Bachman MA.
397 2016. Molecular Epidemiology of Colonizing and Infecting Isolates of Klebsiella
398 pneumoniae. mSphere 1:e00261-16.

399 3. Papazian L, Klompas M, Luyt CE. 2020. Ventilator-associated pneumonia in adults: a
400 narrative review. Intensive Care Med 46:888-906.

401 4. Weiner LM, Webb AK, Limbago B, Dudeck MA, Patel J, Kallen AJ, Edwards JR, Sievert
402 DM. 2016. Antimicrobial-Resistant Pathogens Associated With Healthcare-Associated
403 Infections: Summary of Data Reported to the National Healthcare Safety Network at the
404 Centers for Disease Control and Prevention, 2011-2014. Infect Control Hosp Epidemiol
405 37:1288-1301.

406 5. Gorrie CL, Mirceta M, Wick RR, Edwards DJ, Thomson NR, Strugnell RA, Pratt NF,
407 Garlick JS, Watson KM, Pilcher DV, McGloughlin SA, Spelman DW, Jenney AWJ, Holt
408 KE. 2017. Gastrointestinal Carriage Is a Major Reservoir of Klebsiella pneumoniae
409 Infection in Intensive Care Patients. Clin Infect Dis 65:208-215.

410 6. Adler A, Katz DE, Marchaim D. 2020. The Continuing Plague of Extended-Spectrum β-
411 Lactamase Producing Enterbacterales Infections: An Update. Infect Dis Clin North Am
412 34:677-708.

413 7. Fu M, Blackshear PJ. 2017. RNA-binding proteins in immune regulation: a focus on CCCH
414 zinc finger proteins. Nat Rev Immunol 17:130-143.

415 8. Mino T, Murakawa Y, Fukao A, Vandenbon A, Wessels HH, Ori D, Uehata T, Tartey S,
416 Akira S, Suzuki Y, Vinuesa CG, Ohler U, Standley DM, Landthaler M, Fujiwara T,
417 Takeuchi O. 2015. Regnase-1 and Roquin Regulate a Common Element in Inflammatory
418 mRNAs by Spatiotemporally Distinct Mechanisms. Cell 161:1058-73.
419 9. Matsushita K, Takeuchi O, Standley DM, Kumagai Y, Kawagoe T, Miyake T, Satoh T,
420 Kato H, Tsujimura T, Nakamura H, Akira S. 2009. Zc3h12a is an RNase essential for
421 controlling immune responses by regulating mRNA decay. Nature 458:1185-90.
422 10. Iwasaki H, Takeuchi O, Teraguchi S, Matsushita K, Uehata T, Kuniyoshi K, Satoh T,
423 Saitoh T, Matsushita M, Standley DM, Akira S. 2011. The IκB kinase complex regulates
424 the stability of cytokine-encoding mRNA induced by TLR-IL-1R by controlling
425 degradation of regnase-1. Nat Immunol 12:1167-75.
426 11. Garg AV, Amatya N, Chen K, Cruz JA, Grover P, Whibley N, Conti HR, Hernandez Mir
427 G, Sirakova T, Childs EC, Smithgall TE, Biswas PS, Kolls JK, McGeachy MJ,
428 Kolattukudy PE, Gaffen SL. 2015. MCPIP1 Endoribonuclease Activity Negatively
429 Regulates Interleukin-17-Mediated Signaling and Inflammation. Immunity 43:475-87.
430 12. Tanaka H, Arima Y, Kamimura D, Tanaka Y, Takahashi N, Uehata T, Maeda K, Satoh T,
431 Murakami M, Akira S. 2019. Phosphorylation-dependent Regnase-1 release from
432 endoplasmic reticulum is critical in IL-17 response. J Exp Med 216:1431-1449.
433 13. Uehata T, Iwasaki H, Vandenbon A, Matsushita K, Hernandez-Cuellar E, Kuniyoshi K,
434 Satoh T, Mino T, Suzuki Y, Standley DM, Tsujimura T, Rakugi H, Isaka Y, Takeuchi O,
435 Akira S. 2013. Malt1-Induced Cleavage of Regnase-1 in CD4(+) Helper T Cells Regulates
436 Immune Activation. Cell 153:1036-49.

437 14. Miao R, Huang S, Zhou Z, Quinn T, Van Treeck B, Nayyar T, Dim D, Jiang Z, Papasian
438 CJ, Eugene Chen Y, Liu G, Fu M. 2013. Targeted disruption of MCPIP1/Zc3h12a results
439 in fatal inflammatory disease. Immunol Cell Biol 91:368-76.
440 15. Monin L, Gudjonsson JE, Childs EE, Amatya N, Xing X, Verma AH, Coleman BM, Garg
441 AV, Killeen M, Mathers A, Ward NL, Gaffen SL. 2017. MCPIP1/Regnase-1 Restricts IL-
442 17A- and IL-17C-Dependent Skin Inflammation. J Immunol 198:767-775.
443 16. Li D-D, Bechara R, Ramani K, Jawale CV, Li Y, Kolls JK, Gaffen SL, Biswas PS. 2021.
444 RTEC-intrinsic IL-17–driven inflammatory circuit amplifies antibody-induced
445 glomerulonephritis and is constrained by Regnase-1. JCI Insight 6:e147505.
446 17. Cai S, Batra S, Shen L, Wakamatsu N, Jeyaseelan S. 2009. Both TRIF- and MyD88-
447 dependent signaling contribute to host defense against pulmonary Klebsiella infection. J
448 Immunol 183:6629-38.
449 18. van Lieshout MH, Blok DC, Wieland CW, de Vos AF, van 't Veer C, van der Poll T. 2012.
450 Differential roles of MyD88 and TRIF in hematopoietic and resident cells during murine
451 gram-negative pneumonia. J Infect Dis 206:1415-23.
452 19. Happel KI, Zheng M, Young E, Quinton LJ, Lockhart E, Ramsay AJ, Shellito JE, Schurr
453 JR, Bagby GJ, Nelson S, Kolls JK. 2003. Cutting edge: roles of Toll-like receptor 4 and
454 IL-23 in IL-17 expression in response to Klebsiella pneumoniae infection. J Immunol
455 170:4432-6.
456 20. Ye P, Rodriguez FH, Kanaly S, Stocking KL, Schurr J, Schwarzenberger P, Oliver P,
457 Huang W, Zhang P, Zhang J, Shellito JE, Bagby GJ, Nelson S, Charrier K, Peschon JJ,
458 Kolls JK. 2001. Requirement of interleukin 17 receptor signaling for lung CXC chemokine

459 and granulocyte colony-stimulating factor expression, neutrophil recruitment, and host
460 defense. J Exp Med 194:519-27.
461 21. Aujla SJ, Chan YR, Zheng M, Fei M, Askew DJ, Pociask DA, Reinhart TA, McAllister F,
462 Edeal J, Gaus K, Husain S, Kreindler JL, Dubin PJ, Pilewski JM, Myerburg MM, Mason
463 CA, Iwakura Y, Kolls JK. 2008. IL-22 mediates mucosal host defense against Gram-
464 negative bacterial pneumonia. Nat Med 14:275-81.
465 22. Chen K, Eddens T, Trevejo-Nunez G, Way EE, Elsegeiny W, Ricks DM, Garg AV, Erb
466 CJ, Bo M, Wang T, Chen W, Lee JS, Gaffen SL, Kolls JK. 2016. IL-17 Receptor Signaling
467 in the Lung Epithelium Is Required for Mucosal Chemokine Gradients and Pulmonary
468 Host Defense against K. pneumoniae. Cell Host Microbe 20:596-605.
469 23. Yang C, Huang S, Wang X, Gu Y. 2015. Emerging Roles of CCCH-Type Zinc Finger
470 Proteins in Destabilizing mRNA Encoding Inflammatory Factors and Regulating Immune
471 Responses. Crit Rev Eukaryot Gene Expr 25:77-89.
472 24. Chen K, Eddens T, Trevejo-Nunez G, Way E, Elsegeiny W, Ricks D, Garg A, Erb C, Bo
473 M, Wang T, Chen W, Lee J, Gaffen SL, Kolls J. 2016. IL-17 Receptor Signaling in the
474 Lung Epithelium Is Required for Mucosal Chemokine Gradients and Pulmonary Host
475 Defense against K. pneumoniae. Cell Host Microbe 20:596-605.
476 25. Jeltsch KM, Hu D, Brenner S, Zoller J, Heinz GA, Nagel D, Vogel KU, Rehage N, Warth
477 SC, Edelmann SL, Gloury R, Martin N, Lohs C, Lech M, Stehklein JE, Geerlof A,
478 Kremmer E, Weber A, Anders HJ, Schmitz I, Schmidt-Supprian M, Fu M, Holtmann H,
479 Krappmann D, Ruland J, Kallies A, Heikenwalder M, Heissmeyer V. 2014. Cleavage of
480 roquin and regnase-1 by the paracaspase MALT1 releases their cooperatively repressed
481 targets to promote T(H)17 differentiation. Nat Immunol 15:1079-89.

482 26. Mino T, Murakawa Y, Fukao A, Vandenbon A, Wessels HH, Ori D, Uehata T, Tartey S,
483 Akira S, Suzuki Y, Vinuesa CG, Ohler U, Standley DM, Landthaler M, Fujiwara T,
484 Takeuchi O. 2015. Regnase-1 and Roquin Regulate a Common Element in Inflammatory
485 mRNAs by Spatiotemporally Distinct Mechanisms. Cell 161:1058-1073.
486 27. Akaki K, Ogata K, Yamauchi Y, Iwai N, Tse KM, Hia F, Mochizuki A, Ishihama Y, Mino
487 T, Takeuchi O. 2021. IRAK1-dependent Regnase-1-14-3-3 complex formation controls
488 Regnase-1-mediated mRNA decay. Elife 10.
489 28. Bhat N, Virgen-Slane R, Ramezani-Rad P, Leung CR, Chen C, Balsells D, Shukla A, Kao
490 E, Apgar JR, Fu M, Ware CF, Rickert RC. 2021. Regnase-1 is essential for B cell
491 homeostasis to prevent immunopathology. J Exp Med 218:e20200971.
492 29. Kumaran Satyanarayanan S, El Kebir D, Soboh S, Butenko S, Sekheri M, Saadi J, Peled
493 N, Assi S, Othman A, Schif-Zuck S, Feuermann Y, Barkan D, Sher N, Filep JG, Ariel A.
494 2019. IFN-β is a macrophage-derived effector cytokine facilitating the resolution of
495 bacterial inflammation. Nat Commun 10:3471.
496 30. Akira S. 2013. Regnase-1, a Ribonuclease Involved in the Regulation of Immune
497 Responses. Cold Spring Harb Symp Quant Biol 78:51-60.
498 31. Katakura K, Lee J, Rachmilewitz D, Li G, Eckmann L, Raz E. 2005. Toll-like receptor 9-
499 induced type I IFN protects mice from experimental colitis. J Clin Invest 115:695-702.
500 32. Hamana A, Takahashi Y, Tanioka A, Nishikawa M, Takakura Y. 2018. Safe and effective
501 interferon-beta gene therapy for the treatment of multiple sclerosis by regulating biological
502 activity through the design of interferon-beta-galectin-9 fusion proteins. Int J Pharm
503 536:310-317.

504 33. Xiong H, Carter RA, Leiner IM, Tang YW, Chen L, Kreiswirth BN, Pamer EG. 2015.
505 Distinct Contributions of Neutrophils and CCR2+ Monocytes to Pulmonary Clearance of
506 Different Klebsiella pneumoniae Strains. Infect Immun 83:3418-27.
507 34. Xiong H, Keith JW, Samilo DW, Carter RA, Leiner IM, Pamer EG. 2016. Innate
508 Lymphocyte/Ly6C(hi) Monocyte Crosstalk Promotes Klebsiella Pneumoniae Clearance.
509 Cell 165:679-89.
510 35. Carrero JA, Calderon B, Unanue ER. 2004. Type I interferon sensitizes lymphocytes to
511 apoptosis and reduces resistance to Listeria infection. J Exp Med 200:535-40.
512 36. Martin FJ, Gomez MI, Wetzel DM, Memmi G, O'Seaghdha M, Soong G, Schindler C,
513 Prince A. 2009. Staphylococcus aureus activates type I IFN signaling in mice and humans
514 through the Xr repeated sequences of protein A. J Clin Invest 119:1931-9.
515 37. Boxx GM, Cheng G. 2016. The Roles of Type I Interferon in Bacterial Infection. Cell Host
516 Microbe 19:760-9.
517 38. Ivin M, Dumigan A, de Vasconcelos FN, Ebner F, Borroni M, Kavirayani A,
518 Przybyszewska KN, Ingram RJ, Lienenklaus S, Kalinke U, Stoiber D, Bengoechea JA,
519 Kovarik P. 2017. Natural killer cell-intrinsic type I IFN signaling controls Klebsiella
520 pneumoniae growth during lung infection. PLoS Pathog 13:e1006696.
521 39. Ip WKE, Hoshi N, Shouval DS, Snapper S, Medzhitov R. 2017. Anti-inflammatory effect
522 of IL-10 mediated by metabolic reprogramming of macrophages. Science 356:513-519.
523 40. Sabatel C, Radermecker C, Fievez L, Paulissen G, Chakarov S, Fernandes C, Olivier S,
524 Toussaint M, Pirottin D, Xiao X, Quatresooz P, Sirard JC, Cataldo D, Gillet L, Bouabe H,
525 Desmet CJ, Ginhoux F, Marichal T, Bureau F. 2017. Exposure to Bacterial CpG DNA

526 Protects from Airway Allergic Inflammation by Expanding Regulatory Lung Interstitial
527 Macrophages. Immunity 46:457-473.
528 41. Reich NC. 2013. A death-promoting role for ISG54/IFIT2. J Interferon Cytokine Res
529 33:199-205.
530 42. Yang Z, Liang H, Zhou Q, Li Y, Chen H, Ye W, Chen D, Fleming J, Shu H, Liu Y. 2012.
531 Crystal structure of ISG54 reveals a novel RNA binding structure and potential functional
532 mechanisms. Cell Res 22:1328-38.
533 43. Voll RE, Herrmann M, Roth EA, Stach C, Kalden JR, Girkontaite I. 1997.
534 Immunosuppressive effects of apoptotic cells. Nature 390:350-1.
535 44. von Gamm M, Schaub A, Jones AN, Wolf C, Behrens G, Lichti J, Essig K, Macht A,
536 Pircher J, Ehrlich A, Davari K, Chauhan D, Busch B, Wurst W, Feederle R, Feuchtinger
537 A, Tschöp MH, Friedel CC, Hauck SM, Sattler M, Geerlof A, Hornung V, Heissmeyer V,
538 Schulz C, Heikenwalder M, Glasmacher E. 2019. Immune homeostasis and regulation of
539 the interferon pathway require myeloid-derived Regnase-3. J Exp Med 216:1700-1723.
540 45. Espinosa V, Dutta O, McElrath C, Du P, Chang YJ, Cicciarelli B, Pitler A, Whitehead I,
541 Obar JJ, Durbin JE, Kotenko SV, Rivera A. 2017. Type III interferon is a critical regulator
542 of innate antifungal immunity. Sci Immunol 2.
543 46. Ahn D, Wickersham M, Riquelme S, Prince A. 2019. The Effects of IFN-λ on Epithelial
544 Barrier Function Contribute to Klebsiella pneumoniae ST258 Pneumonia. Am J Respir
545 Cell Mol Biol 60:158-166.
546 47. Carpenter S, Ricci EP, Mercier BC, Moore MJ, Fitzgerald KA. 2014. Post-transcriptional
547 regulation of gene expression in innate immunity. Nat Rev Immunol 14:361-76.

548 48. Li X, Bechara R, Zhao J, McGeachy MJ, Gaffen SL. 2019. IL-17 receptor-based signaling
549 and implications for disease. Nat Immunol 20:1594-1602.
550 49. Sharma P, Allison JP. 2020. Dissecting the mechanisms of immune checkpoint therapy.
551 Nat Rev Immunol 20:75-76.
552 50. Amatya N, EE C, Cruz JA, Aggor F, Garg A, Berman A, Gudjonsson JE, Atasoy U, Gaffen
553 SL. 2018. IL-17 integrates multiple self-reinforcing, feed-forward mechanisms through the
554 RNA-binding protein Arid5a. Science Signaling 11:eaat4617.
555
556
557
558

559 **Figure legends**

560

561 **Figure 1: Reg1-haploinsufficient mice are resistant to KP lung infection.** A) Lung and B)
562 spleen bacterial burdens were assessed by CFU assessment at the indicated time points. Each
563 symbol represents 1 mouse. Filled circle = *Reg1*$^{+/+}$ and open box= *Reg1*$^{+/-}$ mice. C) Weight
564 loss was assessed at the indicated time points (n=15 mice/group). D) Survival of *Reg1*$^{+/-}$ or
565 *Reg1*$^{+/+}$ littermates was assessed up to 8 days post-infection (n=15 mice/group). E) Reg1 gene
566 expression (*Zc3h12a*) in lung homogenates of KP-infected mice. Data are pooled from two
567 experiments. * P<0.05, **<0.01, Log-Rank test. F) Representative images of H&E lung sections
568 from *Reg1*$^{+/+}$ and *Reg1*$^{+/-}$ mice at 48 h post-KP infection. G) Scoring of parenchymal,
569 peribronchial and perivascular inflammation (*Reg1*$^{+/+}$ *n*=6, *Reg1*$^{+/-}$ n=4). * P<0.05, unpaired-t
570 test.

571

572 **Figure 2: Reg1 deficiency in both hematopoietic and non-hematopoietic compartments**
573 **contribute to prolonged survival upon KP lung infection.** A) *Reg1*$^{+/-}$ and *Reg1*$^{+/+}$ littermates
574 were irradiated to ablate bone marrow (BM) and later reconstituted with reciprocal femoral BM
575 cells. Eight weeks after BM transfer, mice were infected with KP and survival monitored over
576 7 days. B) *Reg1*$^{fl/fl}$ were crossed to *Sftpc*^{CreERT2} infected with KP and monitored over 7 d. Data
577 are pooled from two experiments. * P<0.05, **<0.01, Log-Rank test.

578

579 **Figure 3: Immune cell recruitment, proliferation and antibody production are not affected**
580 **by Reg1 deficiency during KP infection.** A-B) Percentage and absolute numbers of cellular
581 recruitment to the lung of infected mice up to 72h post- KP infection. C) BrDU incorporation

582 of lung myeloid cell populations were assessed by flow cytometry at baseline (0 h) or 48 and
583 72 h post-infection. Data are pooled from two independent experiments (A-C). D) Macrophage
584 killing and Ab production in lung was assessed at the indicated time points. Data are pooled
585 from two independent experiments. Data analyzed by one-way ANOVA *P<0.05, ns: not
586 significant.
587
588 **Figure 4: RNASeq of sorted alveolar macrophages reveals an enriched**
589 **Type 1 IFN gene signature.** *Reg1*$^{+/-}$ and *Reg1*$^{+/+}$ littermates were infected with KP or PBS by
590 oropharyngeal aspiration. Alveolar macrophages were sorted by flow cytometry at 24 h post
591 infection and subjected to RNASeq. A) Gene set enrichment analysis (GSEA) of type I IFN
592 gene sets. B) Heatmap depicting differentially expressed genes in the type I IFN pathway (n=4
593 mice/group).
594
595 **Figure 5: Increased IFN-β but not IFN-γ in Reg1 deficient mice during KP infection.**
596 *Reg1*$^{+/-}$ and *Reg1*$^{+/+}$ littermates were infected with KP. A) IFN-β was assessed in lung
597 homogenates by ELISA. B) *Ifnb1* mRNA was assessed in cultured BMDMs infected with heat-
598 killed KP for the indicated time points. C) Levels of IFN-γ were assessed by intracellular
599 staining in total CD45^{+}, NK1.1^{+} and CD4^{+} cells. B) Each symbol represents one mouse.
600 *P<0.05 One-way ANOVA with post-hoc Tukey's test. D) BMDMs were pretreated with LPS for
601 3 h and treated with Act D to stop new transcription. Expression of the indicated mRNAs were assessed
602 for the indicated times by qPCR, normalized to *Gapdh*. Levels compared to time = 0 data are presented
603 as means ± SEM, representative of 2 independent experiments. One-way ANOVA with post hoc
604 Tukey's test *P < 0.05 by; RNA half-life ($t_{½}$) was determined by linear regression as described (50).

605 **Figure 6: IFNR1 blockade in Reg1-deficient mice enhances susceptibility to KP infection.**

606 *Reg1*$^{+/-}$ mice received anti-IFNR1 antibody or isotype control by i.p injection on Day 0 and Day

607 2 post-KP infection. Mice were followed up to 7 days post-infection. (n=5 mice/group).

608 * P<0.05, Log-Rank test.

609

610 **Figure 7: Reg1 deficiency enhances the inflammatory response and increases apoptosis.**

611 A, B) IL-10 and TFNα were assessed by ELISA in lung homogenates of the indicated mice infected

612 with KP. Data are pooled from two independent experiments. C) *Reg1*$^{+/-}$ and *Reg1*$^{+/+}$ littermates

613 were infected with KP. Mice were sacrificed at 48h post-infection, and cleaved Caspase 3 and total

614 Caspase were assessed in lung homogenates by immunoblotting. At right, quantified band intensity

615 values ± SEM is shown. Data are representative of individual replicates.

616

617 **Figure S1: Expression of chemokines and mitochondrial respiration is similar between Reg1**$^{+/-}$

618 **and controls**. *Reg 1*$^{+/-}$ and *Reg1*$^{+/+}$ littermates were given PB or KP by oropharyngeal aspiration and

619 sacrificed at 24h. A) *Cxcl1, Cxcl5* and *Ccl2* expression was measured in lung tissue. Data analyzed by

620 Student t-test and found non-significant B) CD11c^{+} cells sorted from PBS-treated or C) KP-

621 infected mice were sorted and evaluated for oxygen consumption rate (OCR) by Seahorse flux

622 analyzer (n=4 mice per group). Data analyzed by ANOVA and found to be non-significant.

623

624 **Figure S2: Expression of IL-17, IL-22 and IFN-λ are similar between *Reg1*$^{+/-}$ and controls.**

625 *Reg 1*$^{+/-}$ and *Reg1*$^{+/+}$ littermates were infected with KP and sacrificed at the indicated time points. Lung

626 tissues were assessed for protein and mRNA. A) IL-17, B) IL-22, C) IFN-λ, expression in lung

627 homogenates, D) *Regnase-3 (Zc3h12c)* mRNA expression in total lung. Data are pooled from two

628 independent experiments. Data analyzed by ANOVA and found to be non-significant.

629

Figure 1

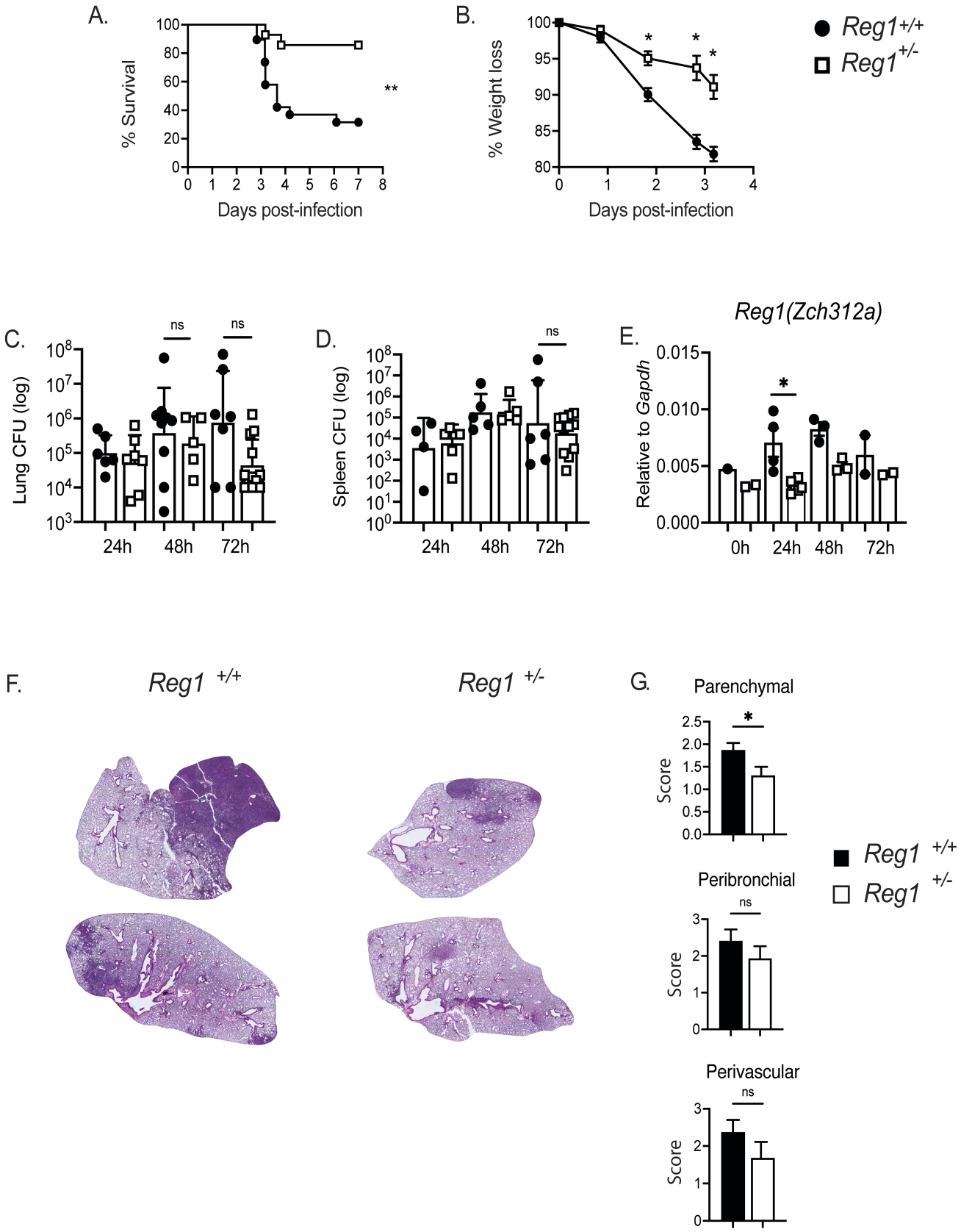
A.
% Survival
Days post-infection
**
B.
% Weight loss
Days post-infection
Reg1+/+
Reg1+/-
C.
Lung CFU (log)
ns
ns
24h
48h
72h
D.
Spleen CFU (log)
ns
24h
48h
72h
E.
Reg1(Zch312a)
Relative to Gapdh
0h
24h
48h
72h
F.
Reg1 +/+
Reg1 +/-
G.
Parenchymal
Peribronchial
Perivascular
Score
ns
Reg1 +/+
Reg1 +/-

Figure 2

A.

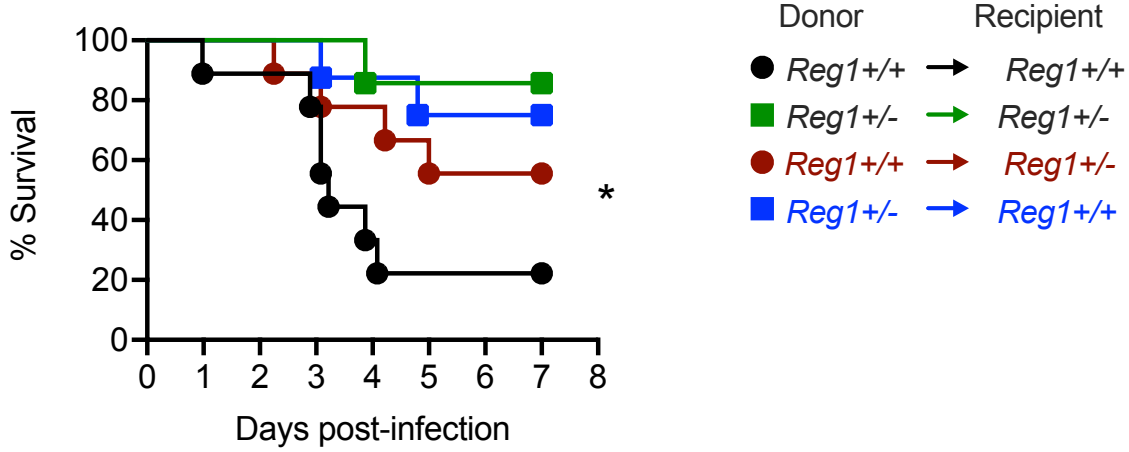
% Survival
100
80
60
40
20
0
0 1 2 3 4 5 6 7 8
Days post-infection
*
Donor
Recipient
Reg1+/+ → Reg1+/+
Reg1+/- → Reg1+/-
Reg1+/+ → Reg1+/-
Reg1+/- → Reg1+/+

B.

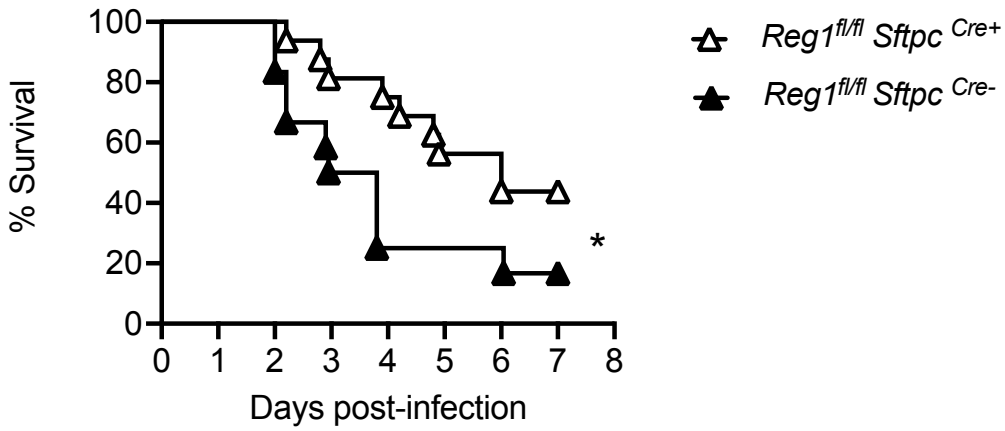
% Survival
100
80
60
40
20
0
0 1 2 3 4 5 6 7 8
Days post-infection
*
Reg1fl/fl Sftpc Cre+
Reg1fl/fl Sftpc Cre-

Figure 3

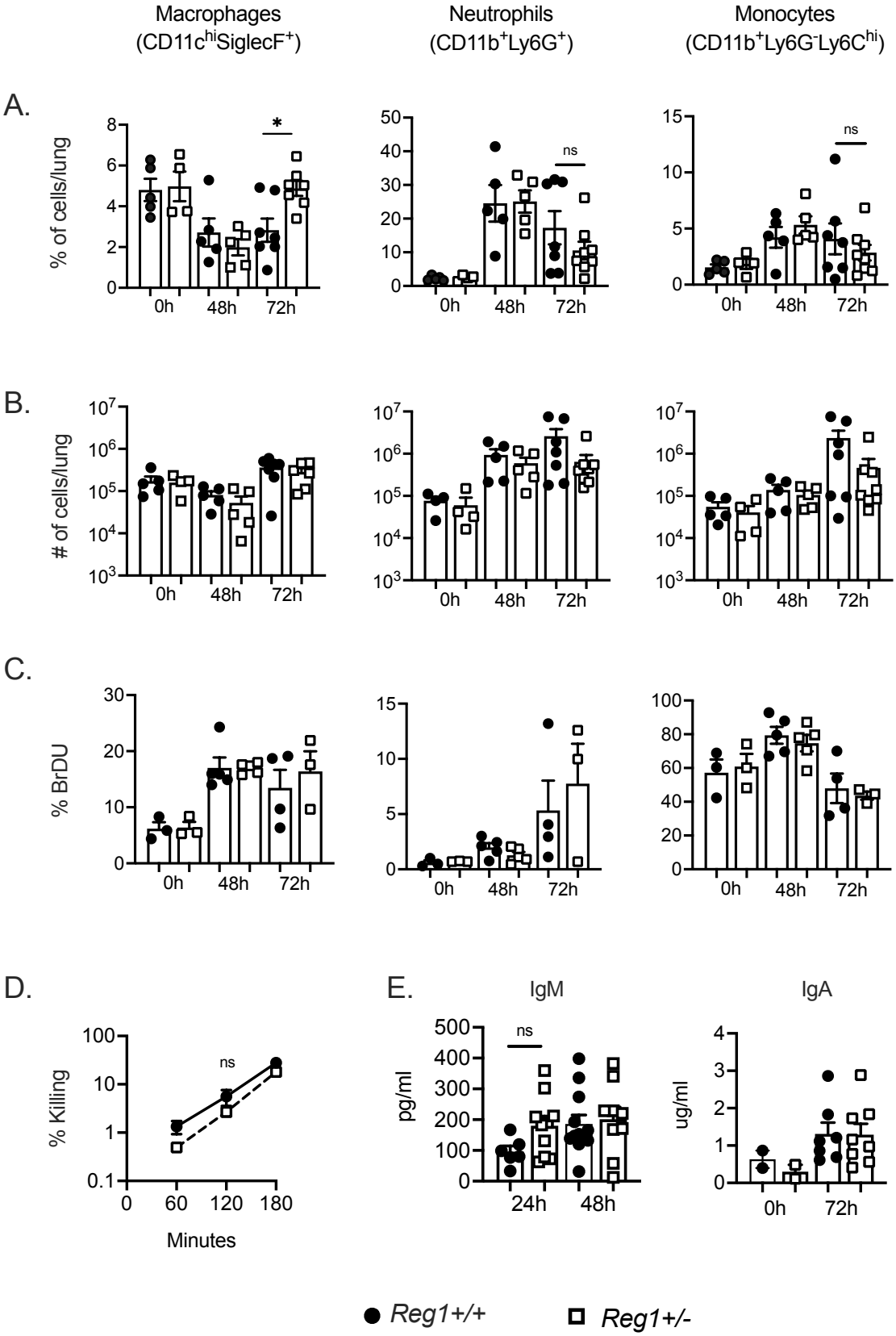
Macrophages
(CD11c^hiSiglecF^+)
Neutrophils
(CD11b^+Ly6G^+)
Monocytes
(CD11b^+Ly6G^-Ly6C^hi)
A.
% of cells/lung
*
ns
ns
0h
48h
72h
B.
# of cells/lung
C.
% BrDU
D.
% Killing
ns
Minutes
E.
IgM
IgA
pg/ml
ug/ml
24h
48h
Reg1+/+
Reg1+/-

Figure 4

A.

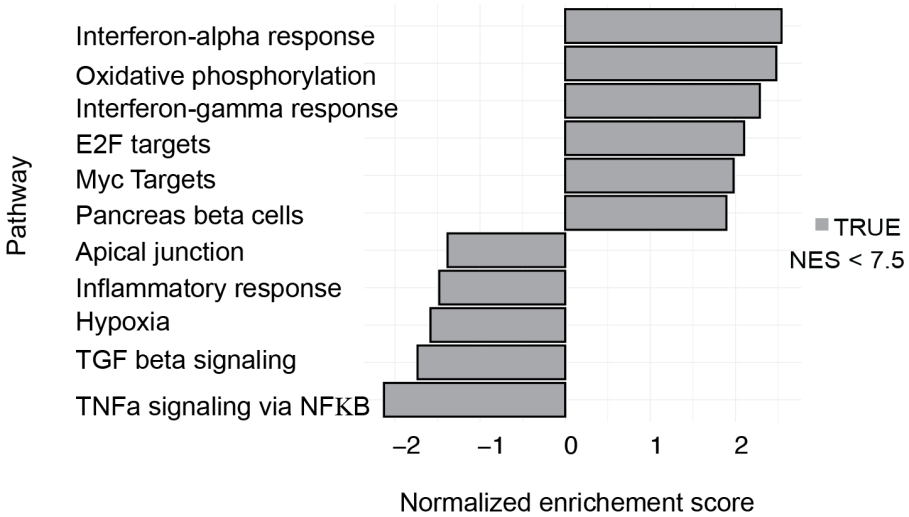
Interferon-alpha response
Oxidative phosphorylation
Interferon-gamma response
E2F targets
Myc Targets
Pancreas beta cells
Apical junction
Inflammatory response
Hypoxia
TGF beta signaling
TNFa signaling via NFKB
Pathway
TRUE
NES < 7.5
−2
−1
0
1
2
Normalized enrichement score

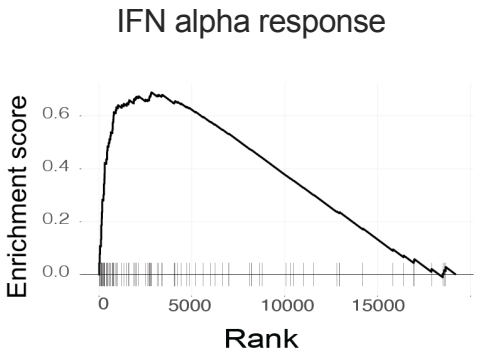
IFN alpha response
Enrichment score
0.6
0.4
0.2
0.0
0
5000
10000
15000
Rank

B.

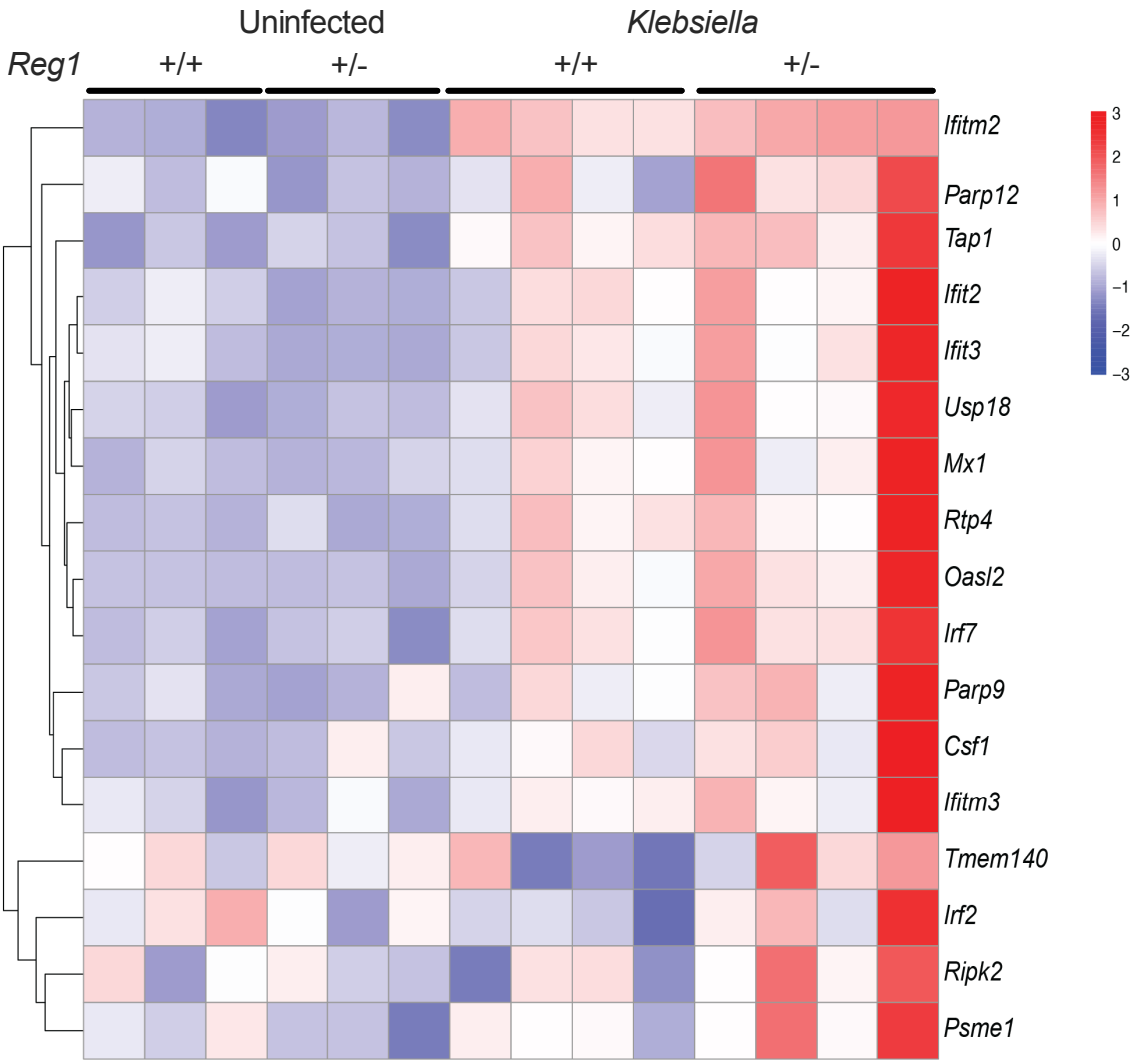
Uninfected
Klebsiella
Reg1
+/+
+/-
+/+
+/-
Ifitm2
Parp12
Tap1
Ifit2
Ifit3
Usp18
Mx1
Rtp4
Oasl2
Irf7
Parp9
Csf1
Ifitm3
Tmem140
Irf2
Ripk2
Psme1
3
2
1
0
−1
−2
−3

Figure 5

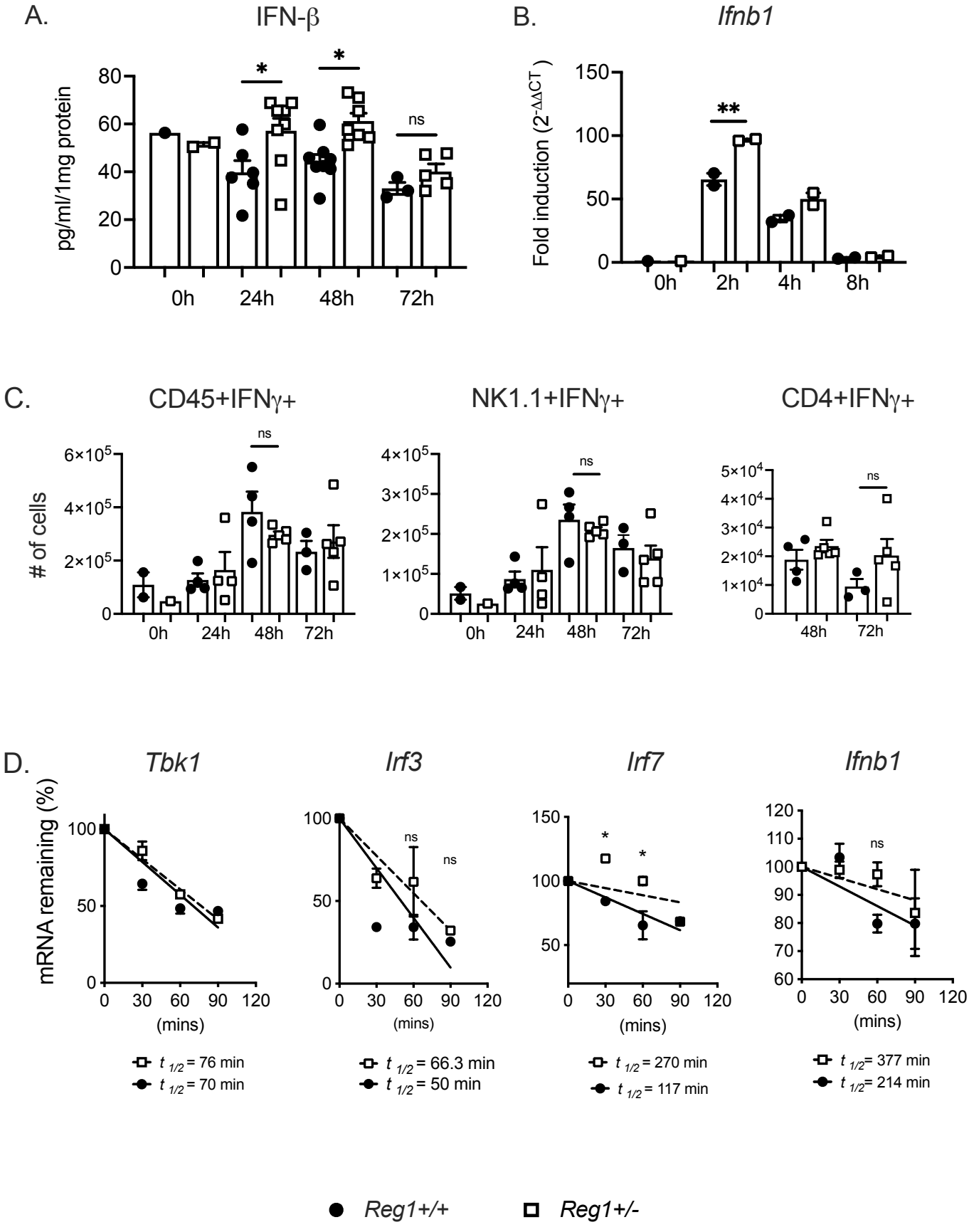
A.
IFN-β
pg/ml/1mg protein
80
60
40
20
0
*
*
ns
0h
24h
48h
72h
B.
Ifnb1
Fold induction (2^-ΔΔCT)
150
100
50
0
**
0h
2h
4h
8h
C.
CD45+IFNγ+
NK1.1+IFNγ+
CD4+IFNγ+
# of cells
6×10^5
4×10^5
2×10^5
0
4×10^5
3×10^5
2×10^5
1×10^5
5×10^4
4×10^4
3×10^4
2×10^4
1×10^4
ns
0h
24h
48h
72h
D.
Tbk1
Irf3
Irf7
Ifnb1
mRNA remaining (%)
(mins)
t 1/2 = 76 min
t 1/2 = 70 min
t 1/2 = 66.3 min
t 1/2 = 50 min
t 1/2 = 270 min
t 1/2 = 117 min
t 1/2 = 377 min
t 1/2 = 214 min
Reg1+/+
Reg1+/-

Figure 6

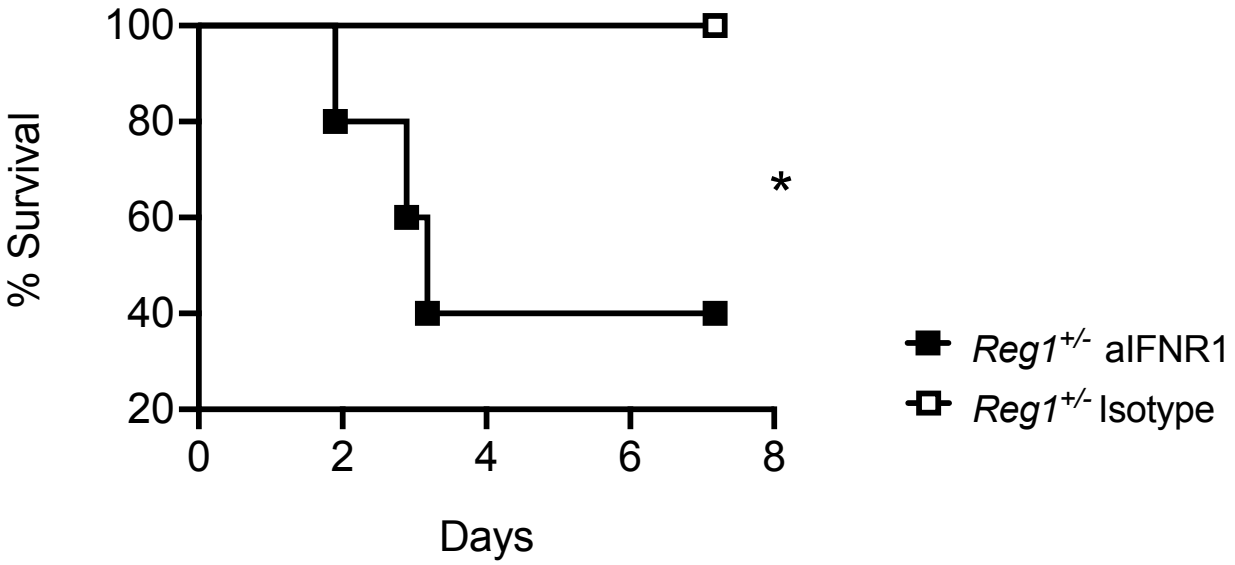

Figure 7

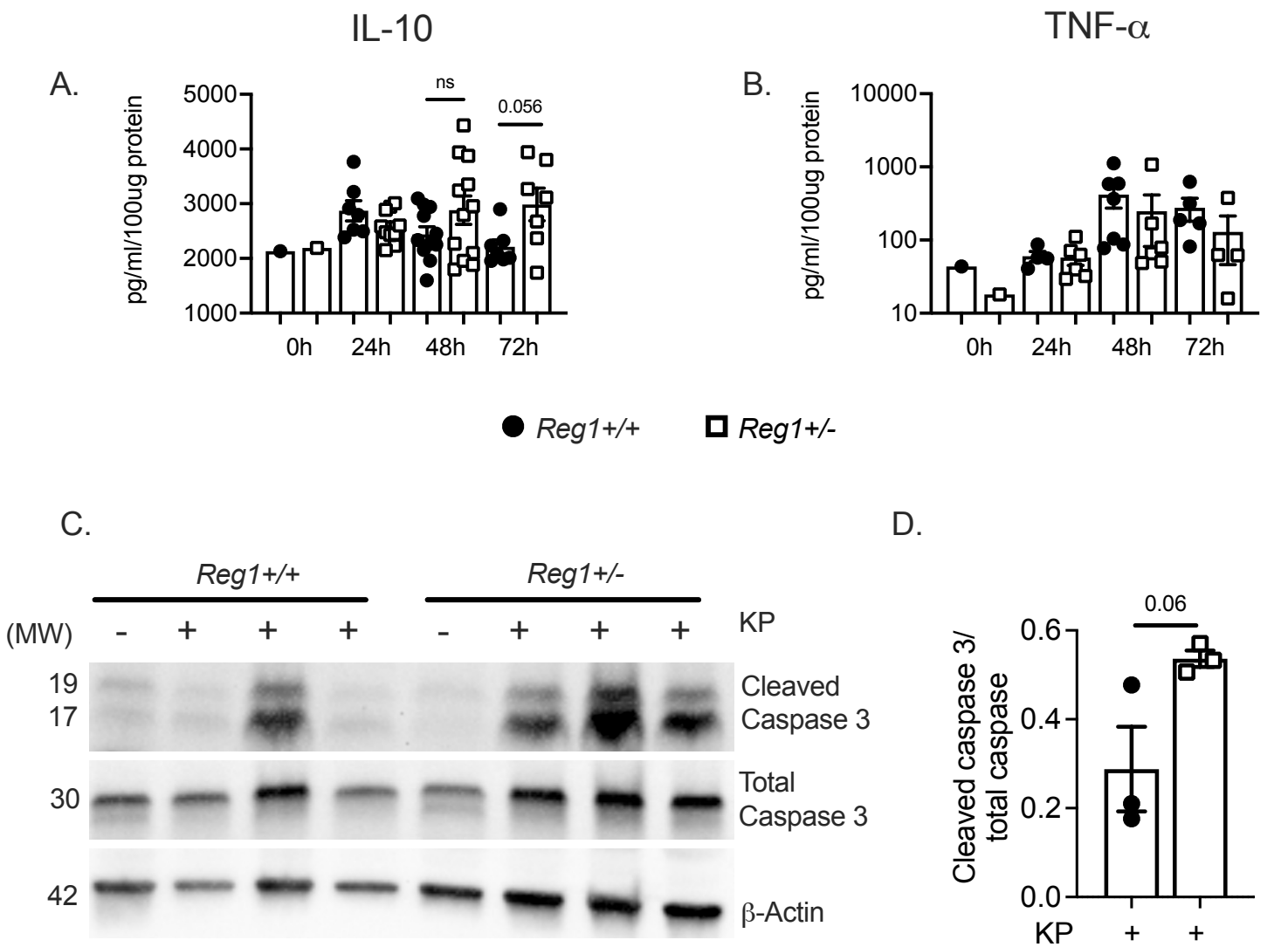
IL-10
A.
pg/ml/100ug protein
5000
4000
3000
2000
1000
ns
0.056
0h
24h
48h
72h
TNF-α
B.
pg/ml/100ug protein
10000
1000
100
10
0h
24h
48h
72h
Reg1+/+
Reg1+/-
C.
Reg1+/+
Reg1+/-
(MW)
- + + +
- + + +
KP
19
17
Cleaved Caspase 3
30
Total Caspase 3
42
β-Actin
D.
0.06
Cleaved caspase 3/ total caspase
0.6
0.4
0.2
0.0
KP
+
+